Received: 17 November 2019 | Revised: 23 March 2020 | Accepted: 13 April 2020

DOI: 10.1002/jbm.b.34620

Society For Biomaterials | WILEY

ORIGINAL RESEARCH REPORT

Microarray analysis reveals that lncRNA PWRN1-209 promotes human bone marrow mesenchymal stem cell osteogenic differentiation on microtopography titanium surface in vitro

Mingyue Wang[1] | Xiyuan Ge[2] | Yan Zheng[1] | Chenxi Wang[1] | Yu Zhang[1] | Ye Lin[1]

[1]Department of Implantology, Peking University School and Hospital of Stomatology & National Clinical Research Center for Oral Diseases & National Engineering Laboratory for Digital and Material Technology of Stomatology & Beijing Key Laboratory of Digital Stomatology, Beijing 100081, People's Republic of China

[2]Central Laboratory, Peking University School and Hospital of Stomatology & National Clinical Research Center for Oral Diseases & National Engineering Laboratory for Digital and Material Technology of Stomatology & Beijing Key Laboratory of Digital Stomatology, Beijing 100081, People's Republic of China

Correspondence
Yu Zhang and Ye Lin, Department of Implantology, Peking University School and Hospital of Stomatology, 22 Zhongguancun South Avenue, Haidian District, Beijing 100081, People's Republic of China.
Email: zhang76yu@163.com (Y. Z.) and yorcklin@263.net (Y. L.)

Funding information
the National Key R&D Program of China, Grant/Award Numbers: 2018YFC1105302, 2018YFC1105304; the Science Foundation of Peking University School and the Hospital of Stomatology (PKUSS), Grant/Award Number: 20150106

Abstract

Sandblasted, large-grit, and acid-etched (SLA) titanium (Ti) with microtopography is currently one of the most widely used implant materials to accelerate osseointegration. Numerous long noncoding RNAs (lncRNAs) have been involved in bone remodeling, with their role in osseointegration, and the underlying mechanisms remain largely unclear. Here, microarrays of human bone marrow mesenchymal stem cells (hBMSCs) were used to identify differentially expressed lncRNAs during early cell differentiation stages (0–7 days) on SLA Ti and polished Ti surfaces. The function of lncRNAs in the osteogenic differentiation of hBMSCs was identified by RNA silencing and overexpression assays. RT-PCR and Western blot were used to detect RNA and protein expression. Alkaline phosphatase (ALP) protein activity was tested by ALP staining. Altogether, 4112 differentially expressed lncRNAs were identified from day 0 to day 7 on SLA Ti with a novel lncRNA, Prader-willi region non-coding RNA 1-209 (PWRN1-209) upregulated. We then proved that PWRN1-209 promoted osteogenic differentiation in hBMSCs by genetic tools. The upregulation of PWRN1-209 was further confirmed to be related to the surface topography of Ti by comparing SLA Ti and polished Ti. Interestingly, this trend seems to have a certain correlation with the mRNA expression level of integrins (α2, αV, β1, β2) and the phosphorylation of focal adhesion kinase (FAK). Taken together, the lncRNA PWRN1-209 was upregulated by the SLA microtopography Ti surface, which may regulate osteogenic differentiation of hBMSCs through integrin-FAK-ALP signaling. Our results provide new insights into the relationship between surface topography and osseointergration.

KEYWORDS

integrin, lncRNA PWRN1-209, microtopography, osteogenic differentiation, titanium

Mingyue Wang and Xiyuan Ge contributed equally to this work.

1 | INTRODUCTION

Rapid and effective osseointegration is critical for the healing of bone with implants. Surface tomography of the implant is one of the six elements of osseointegration (Albrektsson, Brånemark, Hansson, & Lindström, 1981; Branemark, 1983). This characteristic also plays an important role in regulating protein adsorption and cell adhesion by altering intracellular signaling pathways and thus affecting cell phenotype and the overall response to the implant (Cai, Bossert, & Jandt, 2006; Martin et al., 1995; Yang, Wang, Gu, & Leong, 2017). Increasing studies have found that osseointegration is promoted by changing the surface topography and increasing the surface roughness of implants (Boyan et al., 2003; Gittens et al., 2011; Shin et al., 2019). Surface modification by sandblasting with large grit and acid etching (SLA) is the most widely used rough titanium (Ti) implant type clinically. Existing studies have shown that SLA Ti exhibits enhanced osteogenic differentiation with increased levels of specific osteogenic markers and alkaline phosphatase (ALP) and a decreased healing time due to its microscale topography compared to those of a smooth Ti surface (Barbara, 2001; Bornstein et al., 2008; Szmukler-Moncler, Perrin, Ahossi, Magnin, & Bernard, 2004; Wall, Donos, Carlqvist, Jones, & Brett, 2009). However, the molecular mechanisms that enhance osteogenic differentiation and osseointegration after exposure to SLA Ti have not been completely elucidated.

The activation of key regulatory factors is important for the osteogenic process on Ti surfaces. Previous research has elucidated that the gene and protein expression levels varied significantly between SLA Ti surfaces and smooth Ti surfaces, which is due to the interaction within cells and different topography (Barbara, 2001; Wall et al., 2009). Most recent studies have focused on the role of coding genes. Cellular attachment and response to biomaterials are mediated by integrin-extracellular matrix (ECM) proteins (Raines, Berger, Schwartz, & Boyan, 2019). Integrins are transmembrane glycoprotein receptor complexes composed of non-cocalently associated α and β subunits that cluster into focal adhesion kinase (FAK), where they initiate intracellular signaling cascades to regulate the fate of cells (Garcia, 2005; Takeuchi et al., 1997). The expression of α and β subunits is regulated by surface chemistry, topography and hydrophilicity on implant materials. Compared with tissue culture polystyrene (TCPS), the expression of integrin $\alpha 2$ and $\beta 1$ is increased, suggesting that the surface topography-dependent differentiation of osteoblasts is likely to be mediated through $\alpha 2\beta 1$ signaling (Olivares-Navarrete et al., 2008). Cell division cycle 42 (Cdc42) regulates osteogenic differentiation of mesenchymal stem cells (MSCs) on the micro/nano implant surface by GSK3β and Wnt/β-catenin signaling (Li et al., 2017). Studies have shown that rough surface tomography promotes osteogenic differentiation and Wnt/β-catenin signaling pathways (Galli et al., 2010; Wall et al., 2009; Wang et al., 2012). Both the integrin-linked kinase/extracellular signal-related kinase (ILK/ERK) 1/2 and ILK/p38 pathways are involved in promoting osteogenic differentiation by surface tomography of biomaterials (Wang, Liu, Zhang, & Zhao, 2014). Several studies on miRNAs have also been performed. MiR-135b-5p, miR-122-5p, miR-196a-5p, miR-26b-5p, and miR-148b-3p are differentially regulated by surface tomography, and these miRNAs may be involved in differentiation reactions and help regulate the osseointegration process (Sartori et al., 2018). In addition, miR-23a plays a crucial role in the osteogenic differentiation of bone marrow MSCs (BMSCs) cultured on nanostructured Ti by targeting CXCL12 (Zhuang, Zhou, & Yuan, 2019).

LncRNAs are RNA molecules of more than 200 nucleotides in length, accounting for more than 80% of noncoding RNAs, which are widely involved in physiological and pathological processes, including proliferation and migration of tumor cells, tissue and organ development, immune response, and pluripotent stem cell proliferation and differentiation (Batista & Chang, 2013; Fatica & Bozzoni, 2014; Huarte, 2015; J-h et al., 2014). As reported in previous studies, lncRNAs regulate the expression of related target genes at the pretranscriptional, transcriptional, posttranscriptional and epigenetic levels (Li, Wu, Fu, & Han, 2014; Wu et al., 2014). All these characteristics make lncRNA a promising solution for complex physiological processing. However, research on the role of lncRNAs involved in bone regeneration is currently limited. A few lncRNAs, such as H19 (Huang, Zheng, Jia, & Li, 2015; Wu et al., 2018), MEG3(Wang et al., 2017; Zhuang et al., 2015), and DANCR(Tang, Gong, & Sun, 2018; Zhang, Tao, & Wang, 2018), have been reported to participate in the regulation of osteogenic differentiation of MSCs. Nevertheless, the role of lncRNAs in mediating the osteogenic differentiation of human BMSCs (hBMSCs), especially on different topographies (SLA Ti), remains largely unknown.

Here, we identified differentially expressed lncRNAs in hBMSCs after osteogenic induction for 7 or 21 days on the SLA Ti surface by a BeadChip microarray. Ten uncharacterized upregulated lncRNAs were selected in hBMSCs after osteogenic induction at 7 days. After knockdown and overexpression of the lncRNAs in vitro, we detected osteogenesis-related genes and ALP protein activity to explore the effects of the lncRNA on osteogenic differentiation and its possible mechanisms on enhanced differentiation due to increased roughness. We aimed to investigate the response of noncoding RNAs of MSCs to the surface topography of implants, discover novel lncRNAs involved in the osteogenic differentiation of hBMSCs on the microtopography SLA Ti surface and explore the new epigenetic mechanism of enhanced osteogenic differentiation of hBMSCs. This will also help us to understand the role of the implant topography in regulating the cellular response during the complex osseointegration process.

2 | MATERIALS AND METHODS

2.1 | Ti sample preparation

Pure Ti disks (grade 2, purity >99.6%, $34 \times 34 \times 1$ mm^3, Baoji Pengrun New Metal Materials Co., Ltd., Baoji, China) designed for a 6-well plate size were used as samples. The Ti samples were divided into two groups: an SLA Ti disk group (SLA) and a polished Ti disk group (polished Ti). Ti disks were polished with silicon carbide sandpaper of 240–2000 grits, washed with acetone, absolute ethanol and deionized

water for 15 minutes in an ultrasonic cleaner, and then dried at room temperature for 1 hour; these samples comprised the polished Ti group. For the SLA group, the Ti disks were further processed, blasted with aluminum oxide (Al_2O_3) particles, which had a diameter of approximately 0.25–0.5 mm, and etched with a mixture of hydrogen chloride (HCl) and sulfuric acid (H_2SO_4). After etching, Ti samples were cleaned in deionized water within an ultrasonic cleaner for 15 minutes and dried (Wego Jericom Biomaterials Co., Weihai, China). All samples were sterilized in an autoclave (120°C, 30 minutes) before cell plating.

2.2 | Surface characterization

The polished Ti and SLA disks were dried and sprayed with gold, and the surface topography was observed by scanning electron microscopy (SEM; S-4800, Hitachi, Japan) at 15.0 kV. The roughness of the two types of Ti surfaces was evaluated using a 3D optical microscope (CountourGT-K; Bruker, Tucson, AZ). Ra and Sa were selected as the height description parameters. Ra is the arithmetic mean of the absolute deviation from the average line over the length of the samples. Sa is a parameter that is extended by Ra, indicating the average of the absolute values of the height differences of the points with respect to the average surface of the surface.

2.3 | Coding potential analysis

The coding potential of lncRNAs was analyzed by the Coding Potential Assessment Tool (CPAT). (http://lilab.research.bcm.edu/cpat/). Glyceraldehyde-3-phosphate dehydrogenase (Gapdh) and Runx-related transcription factor 2 (Runx2) were used as coding gene controls, and XIST transcripts were used as noncoding gene controls (Zhuang et al., 2018).

2.4 | Cell culture

hBMSCs obtained from ScienCell Company (San Diego, CA) were cultured in growth medium (GM), which is α-MEM supplemented with 10% (v/v) fetal bovine serum (FBS), 100 U/mL penicillin G and 100 mg/mL streptomycin (Gibco, Grand Island, NY). Then, the cells were cultured in a 37°C, 5% CO_2 and 100% relative humidity cell culture incubator. The culture medium was replaced every 2 days. The cells were cultured on TCPS or on Ti disks (SLA, polished Ti disks) at a density of $1 \times 10^4/cm^2$. Cells at passages 4–5 were used for the experiments.

2.5 | Osteogenic differentiation

After hBMSCs were at 70–80% confluence, GM was replaced with osteogenic induction medium (OM) composed of 100 nM dexamethasone, 10 mM β-glycerophosphate and 50 μg/mL ascorbate (Sigma, St. Louis, MO) in addition to GM. OM was replaced every 3 days.

2.6 | ALP staining

After 7 days of osteogenic induction, the medium was aspirated, and the cells were lightly washed 3 times with PBS. After fixation for 30 minutes with 4% paraformaldehyde, the cells were lightly washed three times with PBS for 3 minutes each time. The BCIP/NBT Alkaline Phosphatase Kit (Beyotime, Shanghai, China) was used according to the instructions, and staining was performed in the dark for 30 minutes. After staining, the staining solution was aspirated and washed three times with PBS for 3 minutes each time, and the staining was terminated. The results of the staining were recorded by scanning under a scanner.

2.7 | Microarray analysis

In the previous experiment, we extracted hBMSCs that underwent osteogenic induction on SLA Ti disks for 7 days or 21 days and cultured hBMSCs in GM as a control. The lncRNA microarray data were obtained, and differential expression analysis was performed by R-SEM software to generate a heat map. (To select differentially expressed genes, we used the threshold of |fold change| > 2. The log data were converted and centered using the adjusted data function of CLUSTER 3.0 software (University of Tokyo; Human Genome Center, Tokyo, Japan), and then, further analysis and generation of heat maps were performed using hierarchical clustering with average linkages.) The gene expression profiles were evaluated for further analyses using Excel, SPSS or GraphPad Prism 7.0 software. Selection and verification of the raw data of lncRNAs related to osteogenic differentiation on the SLA Ti surface were performed using Prism7.0 to generate new heat maps representing differentially expressed genes we selected (fold change > 8.0).

2.8 | Quantitative real-time polymerase chain reaction (qRT-PCR): RNA extraction, reverse transcription and real-time PCR

Total RNA was isolated using TRIzol reagent (Invitrogen, Carlsbad, CA) according to the instructions. Then, RNA was reverse transcribed with a PrimeScript TM RT Reagent Kit (TaKaRa, Tokyo, Japan) to obtain cDNA according to the manufacturer's instructions. Quantitative RT-PCR analysis was performed with SYBR Green Master Mix (Roche Applied Science, Mannheim, Germany) using a real-time PCR detection system (Applied Biosystems, Foster City, CA). GAPDH served as an internal reference control. The relative expression levels of mRNA and lncRNA were calculated using the $2^{-\Delta\Delta Ct}$ method. The primer sequences are shown in Table 1.

TABLE 1 Primers used in real-time PCR

Genes	Forward sequence (5′–3′)	Reverse sequence (5′–3′)
Alkaline phosphatase (Alp)	ACTCTCCGAGATGGTGGTGGTG	CGTGGTCAATTCTGCCTCCTTCC
Bone sialoprotein (Bsp)	GTCTATAGAACCACTTCCCCAC	GCTGTACTCATCTTCATAGGCT
Collagen type I a1 (Col1a1)	ATCAACCGGAGGAATTTCCGT	CACCAGGACGACCAGGTTTTC
Runx-related transcription factor 2 (Runx2)	CCATAACGGTCTTCACAAATCCT	TCTGTCTGTGCCTTCTTGGTTC
Glyceraldehyde-3-phosphate dehydrogenase (Gapdh)	GGTCACCAGGGCTGCTTTTA	GGATCTCGCTCCTGGAAGATG
ENST00000506795.1	GCTAGACCAGCCACAGAACTTCC	CTTCCTTCTAGCCACAGAGCCTTG
ENST00000422014.1	ATTATGGATATGTGCCGCCGAAGC	GGACTCAACAGAGCCAAGCCTTG
ENST00000609012.1	TCTCTCCTCTGCCTTCTCCTT	ATCTCGGGTACCAGCACAGT
ENST00000424126.1	GAGTCAGACGCAGAAGCTCG	CCTGACTTGCGCATTGGTCT
ENST00000568730.1	TGTGGGGACACAGAGCCTTA	TGTCCAAATTGCCACGATGTCT
ENST00000426661.1	GGATTCCTCTGCCTGCTGATGC	GTTGAGCTGAGATCCTGCCACTG
ENST00000528383.1	CTTGGCCAGTCAGCCAAGTT	GGCCACATGAGTGGTAGGGA
PWRN1-209	GATGCGATCCAGCCAGTCTGTAC	CAGGCTGTGGTGTGGCATGG
ENST00000547563.1	GAGCGCTCAAGGATGTTGGC	GCAGTCTTCTCTTGATTAGCCATGT
ENST00000518926.1	GTCCACAGGATACCATCACTGAGC	GACTGCTGATTCCTTGGTGTTCC
Integin α2 (Itgα2)	GTCCTGTTGACCTATCCACT	CCACCAGAAGCTGCTGAATA
Integin αv (Itgαv)	TGCAGTGTGAGGCTGTGTACA	GTGGCCACCTGACGCTCT
Integin β1 (Itgβ1)	GCGAAGGCATCCCTGAAAGT	GGACACAGGATCAGGTTGGA
Integin β2 (Itgβ2)	GCGTGACATTCCAATCAGGGA	AGAGAGGACCCCAGTGGCAA

2.9 | Knockdown assay

Small interfering RNAs (siRNAs) specifically targeting lncRNAs (si-ENST00000422014.1, si-ENST00000528383.1, si-ENST00000547563.1, si-ENST00000518926.1, si-PWRN1-209, si-ENST00000568730.1, si- ENST00000506795.1), scrambled siRNA (NC) and FAM siRNA were designed and synthesized by Shanghai GenePharma (Shanghai, China). The hBMSCs were plated in 6-well plates and 12-well plates before transfection at a density of $2 \times 10^4/cm^2$. When the cells were grown to 70–90% confluence, the siRNA was transfected into the cells by Lipo3000 (Invitrogen, CA) within 24 hours after plating, and total RNA was extracted at 48 hours. The efficiency of transfection and knockdown was detected by fluorescence microscopy and qRT-PCR. On day 7, ALP staining and qRT-PCR were performed to detect the expression of osteogenic genes. Transfection was performed every 3 days. All siRNA sequences are shown in Table S1.

2.10 | Overexpression assay

The lncRNA complementary DNA (cDNA) sequences were synthesized and cloned into the pcDNA3.1(+) vector (Invitrogen, Shanghai, China), and the recombinant vectors were named oeENST00000528383.1, oePWRN1-209, oeENST00000518926.1, and oeENST00000568730.1. An empty pcDNA3.1(+) vector was used as the control, named Vec. The cells were plated in 6-well plates and 12-well plates for 24 hours before transfection at a density of $2 \times 10^4/cm^2$. The cells were grown to 70%–90% confluence when the plasmids were transfected into cells using TransIT-2020 Transfection reagent (Mirus, MA) within 24 hours after plating, and RNA was isolated to detect the overexpression efficiency at 48 hours by qRT-PCR. After 7 days, ALP staining and qRT-PCR were performed to detect the expression of osteogenic genes.

2.11 | Western blot

Western blotting was performed as described previously. Briefly, cells were lysed in radioimmunoprecipitation assay (RIPA) buffer containing a protease inhibitor cocktail (Solarbio, China). A BCA protein kit was used to quantify each group of cell lysates. Equal amounts of protein mixed with loading buffer (Solarbio, China) were separated on 10% sodium dodecyl sulfate-polyacrylamide gels for electrophoresis, and the proteins were transferred onto a polyvinylidene fluoride membrane (Millipore, MA) for immunoblotting. Then, the membrane was incubated with primary antibodies against ALP, β-actin, p-FAK (pY397), and FAK (Cell Signaling Technology) overnight at 4°C. After washing 3 times, the membrane was incubated with secondary antibodies (Cell Signaling Technology) and visualized using an ECL Western Blot Kit (CWBIO, China). ImageJ software was used to measure the gray value of each target band.

2.12 | Statistical analysis

Statistical analysis was performed using SPSS 25.0, and the statistical significance of the comparison between the two groups was determined by Student's *t* test. A two-tailed *p* value <0.05 was considered statistically significant (*$p < 0.05$; **$p < 0.01$). The results represent the mean of three independent experiments, and the data are expressed as the mean ± *SD*. Figures were generated using GraphPad Prism 7 software (GraphPad Software, Inc., La Jolla, CA).

3 | RESULTS

3.1 | Characterization of SLA Ti and polished Ti

The topographies of the SLA Ti disks and the polished Ti disks were characterized by SEM (Figure 1a and Figure S1A). The SLA Ti surface exhibited a typical surface tomography of an SLA-type implant obtained by a sandblasting and acid etching process. In addition, SLA Ti exhibited a layered and complex porous appearance, which was a crater-like depression with a diameter of several micrometers to several tens of micrometers and microscale micropores. The polished Ti was relatively smooth and had parallel scratches. A 3D optical microscope showed that the average Ra value of the SLA Ti surface was 1.8 μm, and the average Sa was 1.8 μm (Figure 1b,c). The polished Ti had a Ra value of 0.2 μm and an average Sa value of 0.2 μm (Figure S1B).

3.2 | Morphology and osteogenic differentiation of hBMSCs

As shown in Figure S2A, hBMSCs at the fifth passage exhibited a spindle-like morphology. First, we evaluated the osteogenic differentiation ability of purchased hBMSCs under osteogenic induction conditions by culturing cells in GM or OM for 7 days. After osteogenic induction, qRT-PCR showed that the expression levels of the osteogenic genes Alp, Bone sialoprotein (Bsp), Collagen type I a1 (Col1a1), and Runx2 in hBMSCs were increased by 10.9-, 20.1-, 1.6-, and 6.4-fold, respectively (Figure S2B). ALP staining revealed a significant increase in ALP protein activity following osteogenic induction (Figure S2C). Consequently, our data demonstrated the osteogenic differentiation ability of our hBMSCs in the osteogenic culture used in this study.

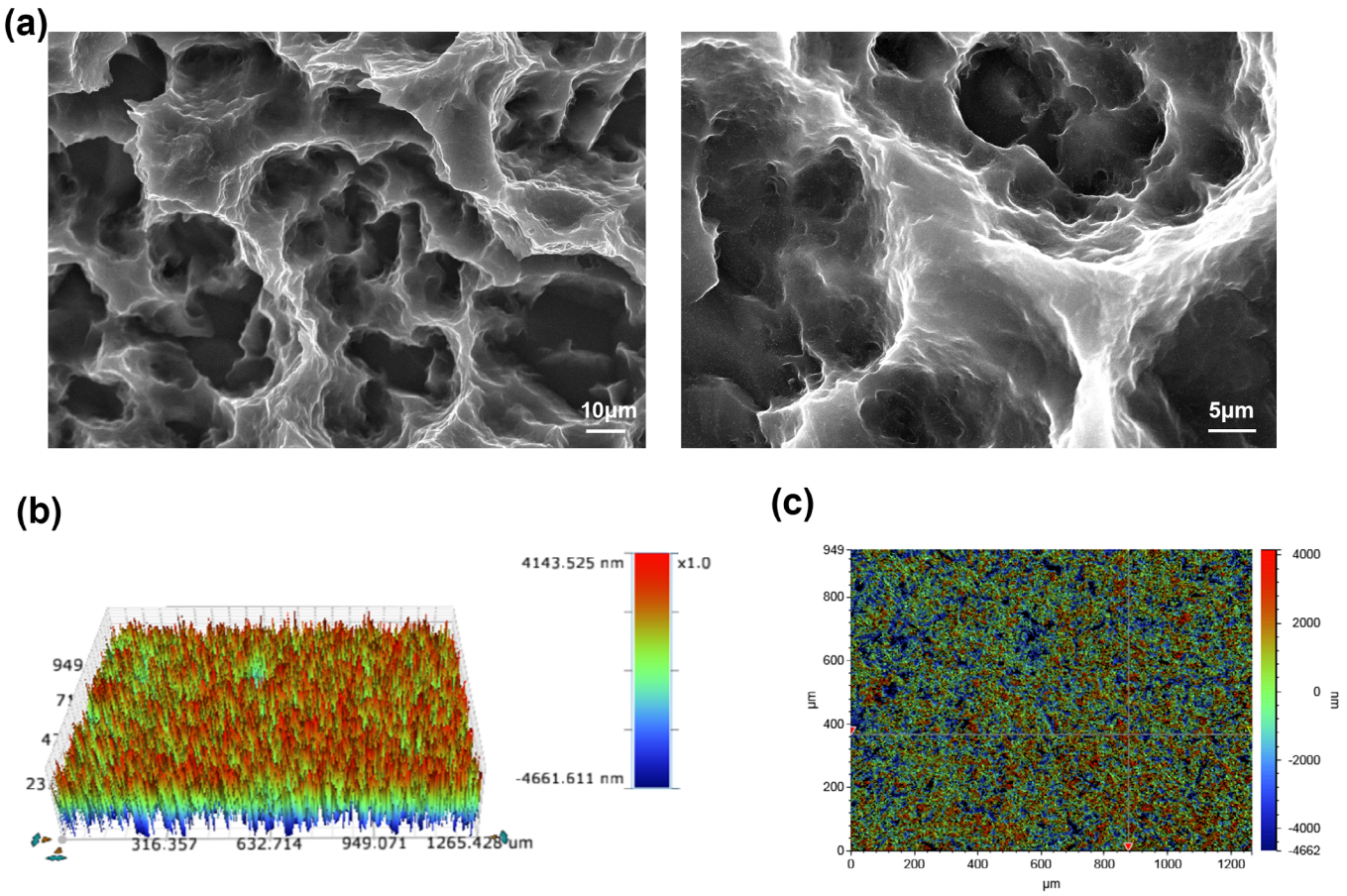

FIGURE 1 Surface characterization. (a) Characterizing the SLA titanium surface by SEM at different magnifications. (b), (c) 3D optical microscope characterizing the SLA titanium surface

3.3 | Differentially expressed lncRNA selection by microarray and verification by qRT-PCR

To identify lncRNAs that were involved in the osteogenic differentiation of hBMSCs on SLA Ti, we performed lncRNA microarrays using RNA extracted from hBMSCs cultured in OM on SLA for 0, 7, or 21 days. To our surprise, we found that many uncharacterized lncRNAs correlated with osteogenesis in SLA. The heat map in Figure 2a and Figure S3A shows the differentially expressed lncRNAs. After osteogenic differentiation on SLA Ti, 2858 upregulated lncRNAs and 1254 downregulated lncRNAs were found on day 7, while 1437 differentially expressed lncRNAs were found at 21 days, indicating that most of the changes in lncRNA expression were mainly in the stage of early osteogenic differentiation (Figure S3C). Therefore, we focused on the top 10 uncharacterized upregulated lncRNAs (fold change > 8.0) selected from the lncRNA microarray data on day 7, and a heat map was generated (Figure 2b and Table S2). We also performed a heat map of these ten lncRNAs of microarray data on day 21 (Figure S3B and Table S2, six lncRNAs of ten on day 21 were undetected because of low expression level). We verified by qRT-PCR that seven lncRNAs, including ENST00000506795.1, ENST00000547563.1, Prader-willi region non-coding RNA1-209 (PWRN1-209, gene symbol: ENST00000566676.1), ENST0000051 8926.1, ENST00000422014.1, ENST00000568730.1, and ENST00 000528383.1, were upregulated after osteogenic induction on SLA Ti on day 7 (Figure 2c).

3.4 | Knockdown of lncRNAs

To explore the physiological effect of these seven lncRNAs in osteogenic differentiation, we silenced the corresponding lncRNAs in hBMSCs using siRNAs.

3.4.1 | Transfection efficiency

The transfection efficiency of hBMSCs was confirmed to be over 70% by FAM siRNA transfection (Figure 3).

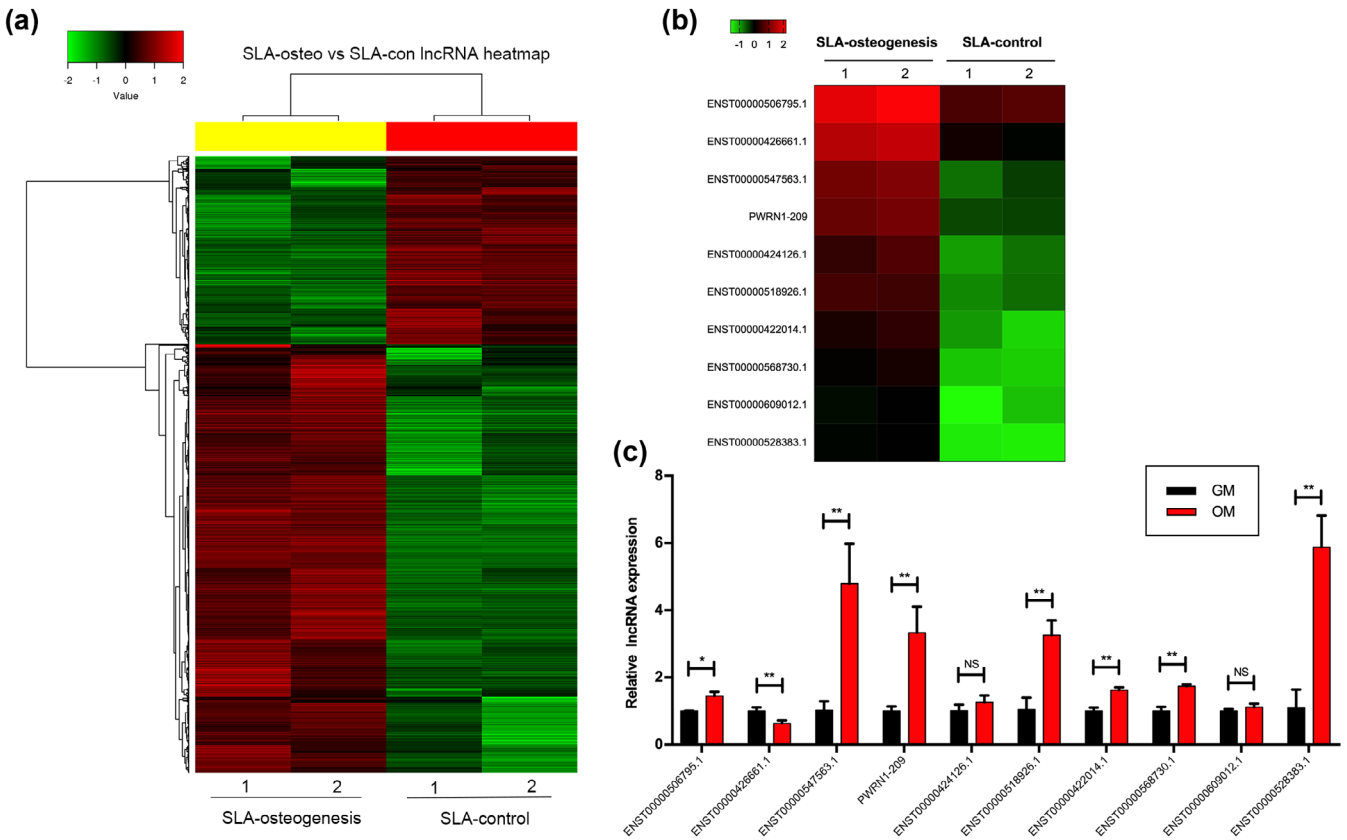

FIGURE 2 LncRNAs were upregulated in hBMSCs after osteoinduction on SLA at 7 days. (a) Clustering heat map of 4112 differentially expressed lncRNAs analyzed by microarray analysis of hBMSCs cultured in osteogenic induction medium (OM) versus growth medium (GM) on SLA Ti at 7 days. (b) Heatmap showing ten upregulated lncRNAs (fold change>8) on SLA Ti after osteogenic induction. Red indicates high expression, and green indicates low expression. Each column represents one sample, and each row represents one lncRNA. (c) Verification of ten uncharacterized differentially expressed lncRNAs by qRT-PCR at 7 days. (Error bars are the mean ± *SD*, $^{*}p < 0.05$; $^{**}p < 0.01$, ns means no significant difference, $n = 3$)

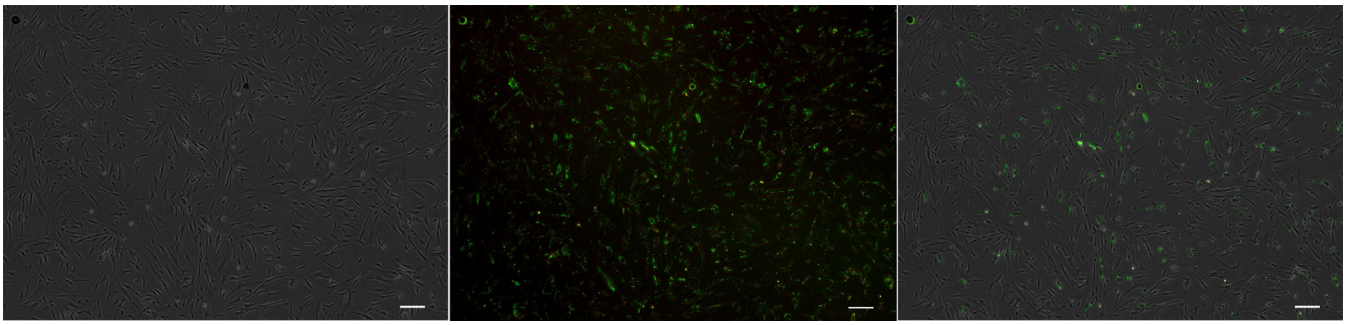

FIGURE 3 Fluorescent photomicrographs showing that the efficiency of FAM-siRNA transduction was over 70% in hBMSCs after 24 hours (scale bar = 200 μm)

3.4.2 | Expression of osteogenic markers

The knockdown efficiency was confirmed by qRT-PCR. Except for the knockdown efficiency of ENST00000547563.1 and ENST00000506795.1, which was less than 70%, the knockdown efficiencies of the other five lncRNAs were over 70% (Figure 4a and Figures S4A, S5A, S6A, S7A, S8A and S9A).

We evaluated the mRNA expression of several osteogenic markers by qRT-PCR. We found that PWRN1-209 depletion downregulated Alp, Bsp and Col1a1 mRNA expression (Figure 4b), while the expression of Runx2 mRNA showed no significant difference. Knockdown of ENST00000547563.1 only downregulated Runx2 mRNA expression and upregulated Alp and Bsp mRNA expression compared to those of the NC group after 7 days in OM (Figure S4B); knockdown of

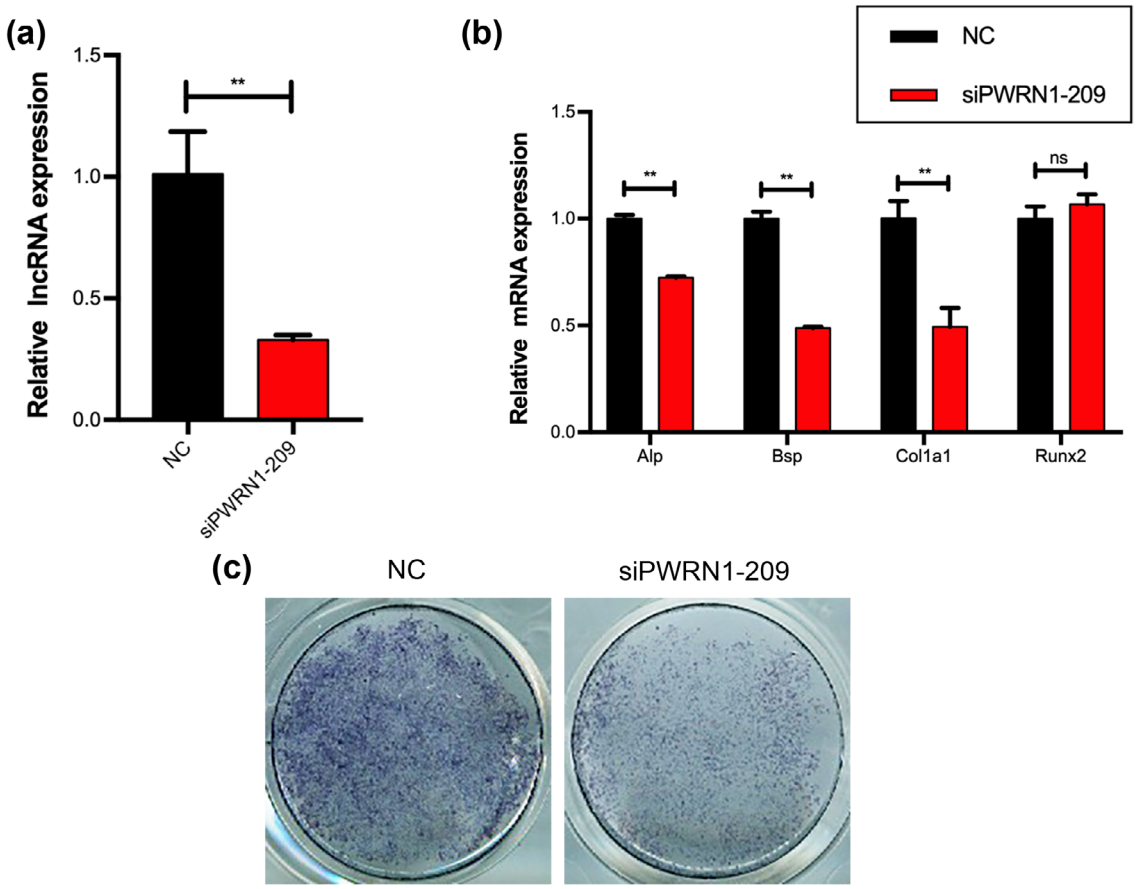

FIGURE 4 Knockdown of PWRN1-209 suppresses the osteogenic differentiation of hBMSCs in vitro. (a) SiRNA knockdown efficiency of PWRN1-209 in hBMSCs. (b) Relative mRNA expression of alkaline phosphatase (Alp), bone sialoprotein (Bsp), collagen type I a1 (Col1a1) and runt-related transcription factor 2 (Runx2) was measured by qRT-PCR at day 7 of osteogenic induction (error bars are the mean ± *SD*, $^{*}p < 0.05$; $^{**}p < 0.01$, ns indicates no significant difference, $n = 3$). (c) ALP staining was used to characterize the expression level of ALP protein after knockdown of PWRN1-209

ENST00000422014.1 and ENST00000568730.1 suppressed the mRNA levels of Alp, Bsp and Runx2 (Figure S5B and S6B); ENST00000528383.1 depletion downregulated Alp, Bsp, Col1a1, and Runx2 mRNA expression (Figure S7B); and knockdown of ENST00000518926.1 only downregulated Alp and Col1a1 mRNA expression compared to that of the NC group (Figure S8B). Knockdown of ENST00000506795.1 increased the mRNA levels of Alp and Bsp (Figure S9B).

3.4.3 | ALP activity

Notably, compared with that of the NC group, ALP protein activity was significantly downregulated by knockdown of PWRN1-209, ENST00000547563.1, ENST00000422014.1, ENST00000528383.1, ENST00000518926.1, or ENST00000568730.1, which dramatically suppressed osteogenic differentiation in OM for 7 days (Figure 4c and Figures S4C, S5C, S6C, S7C, and S8C). However, silencing ENST00000506795.1 failed to influence ALP activity (Figure S9C).

Regarding qRT-PCR and ALP staining results, we presumed PWRN1-209, ENST00000422014.1, ENST00000528383.1, ENST00000518926.1, and ENST00000568730.1 among the lncRNAs may promote osteogenic differentiation of hBMSCs in vitro.

3.5 | Overexpression of lncRNAs

To further confirm the role of the above lncRNAs in the osteogenic differentiation of hBMSCs, we selected four lncRNAs that dramatically suppressed osteogenic differentiation when knocked down. The corresponding lncRNAs were then overexpressed in hBMSCs by plasmid transfection.

3.5.1 | Expression of osteogenic markers

The overexpression efficiency was confirmed by qRT-PCR (Figure 5a and Figures S10A, S11A, and S12A). We evaluated the expression of several osteogenic markers as before. Consistently, PWRN1-209 overexpression enhanced the mRNA levels of the osteogenic differentiation genes Alp, Bsp, and Col1a1 compared to those of the empty vector-transfected hBMSCs (Figure 5b). Overexpression of

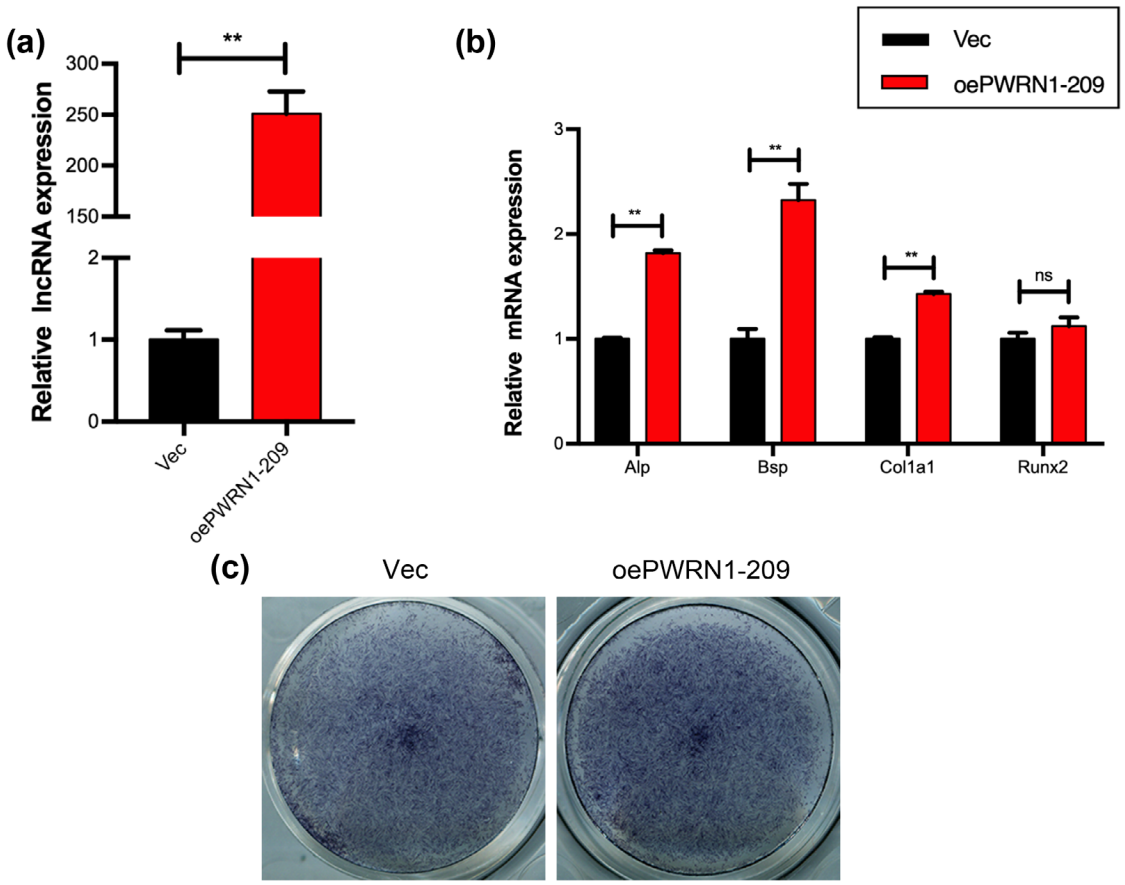

FIGURE 5 The effect of PWRN1-209 overexpression in hBMSCs in vitro. (a) Overexpression efficiency of lncRNAs in hBMSCs with plasmid transfection. (Vec served as an empty vector negative control); (b) Relative mRNA expression of alkaline phosphatase (Alp), bone sialoprotein (Bsp), collagen type I a1 (Col1a1) and runt-related transcription factor 2 (Runx2) was measured by qRT-PCR at day 7 of osteogenic induction (error bars are the mean ± *SD*, *$p < 0.05$; **$p < 0.01$, ns means no significant difference, $n = 3$). (c) ALP staining was used to characterize the expression level of ALP protein overexpression of PWRN1-209

ENST00000528383.1 only upregulated Alp and Co1a1 mRNA expression (Figure S10B), and overexpression of ENST00000518926.1 and ENST00000568730.1 augmented the mRNA expression of Alp, Bsp, Col1a1, and Runx2 (Figures S11B and S12B).

3.5.2 | ALP activity

Only PWRN1-209 overexpression enhanced the ALP protein activity of hBMSCs, as shown by ALP staining, compared with that of vector-transfected hBMSCs (Figure 5c and Figures S10C, S11C, and S12C).

While ENST00000528383.1, ENST00000518926.1, and ENST00000568730.1 resulted in slightly lower ALP protein levels than the vector-transfected group, as measured by ALP staining, there was a large difference in osteogenic differentiation gene expression. One might expect differences at the gene and protein levels. This result motivated our interest in better characterizing and quantifying the phenotype through multiple measures.

Collectively, through further overexpression experiments, we concluded that PWRN1-209, which is upregulated by osteoinduction on microtopography SLA Ti, likely drives the osteogenic differentiation of hBMSCs in vitro.

3.6 | CPAT analysis of PWRN1-209

Then, we performed CPAT coding potential analysis (Figure 6), and the results showed that PWRN1-209 did not encode proteins.

3.7 | Differential expression of PWRN1-209 and consistency with the expression trend of integrins and FAK on different topography surfaces

At day 7, 510 upregulated lncRNAs and 622 downregulated lncRNAs were found on SLA versus polished ti surface after osteoinduction (Figure 7a), which showed that topography affected the expression level of lncRNAs. Since we have already proven the positive effect of PWRN1 on hBMSC osteogenic differentiation, upregulating the expression of ALP/Alp, but not Runx2, this effect may be connected with topography. To further explore the possible mechanisms of PWRN1-209 on osteogenic differentiation, we analyzed the effect of surface topography on the expression of integrins. The expression levels of itgα2, itgαv, itgβ1, and itgβ2 on TCPS, polished Ti and SLA surfaces in hBMSCs are shown in Figure 7b-e. Significant increases in the expression of α2, αv, β1, and β2 were observed on the rough topography SLA surface versus polished Ti, which was also higher than TCPS. Interestingly, we found that PWRN1-209 increased over two-fold on TCPS after osteoinduction (Figure 7f). Additionally, this lncRNA was upregulated on the surface of titanium material and was affected by the roughness of the material, and its expression level was higher on the enhanced rough SLA Ti surface than on the polished Ti surface (Figure 7f). This result indicated that PWRN1-209 may be affected by titanium and the microtopography of SLA, and there is a certain connection between the expression of integrins and lncRNA PWRN1-209, which may be involved in microtopographically improved osteogenic differentiation. Western blot results showed the content of FAK phosphorylation and ALP protein in hBMSCs on diverse surfaces, which suggested that SLA with microtopography induced a high level of p-FAK as well as ALP. The level of p-FAK was higher than that on polished Ti and 2 times higher than that on TCPS (Figure 7g–j).

The consistency with the expression trend of integrins and FAK of PWRN1-209 on several topography surfaces suggests that lncRNA PWRN1-209 was likely to promote BMSC osteogenic differentiation in FAK-mediated signal transduction via cell surface ECM interaction of rough topography and trigger ALP gene expression via integrin-mediated FAK activation which was similar to the effect of osteopontin (OPN) to promote early-stage osteogenic differentiation of hBMSCs (Liu et al., 1997).

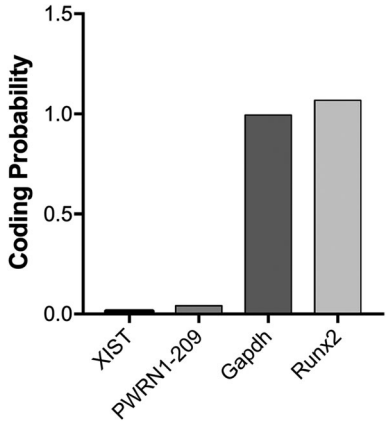

FIGURE 6 Coding potential analysis of PWRN1-209

4 | DISCUSSION

LncRNA is an emerging regulator with a prominent variety of biological functions that plays a crucial role in RNA-related regulation within miRNAs and mRNAs. In recent years, increased attention has been paid to the mechanism by which lncRNAs regulate stem cell differentiation. Many studies have verified that numerous identified lncRNAs play important roles in MSC osteogenic differentiation (Tang et al., 2019; Yang et al., 2018; Zhang et al., 2017). There has been little research on the role of lncRNAs in regulating cellular responses during complex osseointegration on the surface of titanium. Jin et al found that lncRNA CCL3-AS could enhance the cell viability of MSCs and inhibit osteogenic differentiation on TiO_2 nanotube (TNT) substrates in the early stage (Jin et al., 2019). However, no studies have been reported on the lncRNA mechanism and the upstream/downstream signaling pathways that promote osteogenic differentiation and osseointegration on the microtopography SLA Ti surface. Therefore, the mechanism of how BMSCs are affected by lncRNAs on the microtopography surface is eager to be revealed.

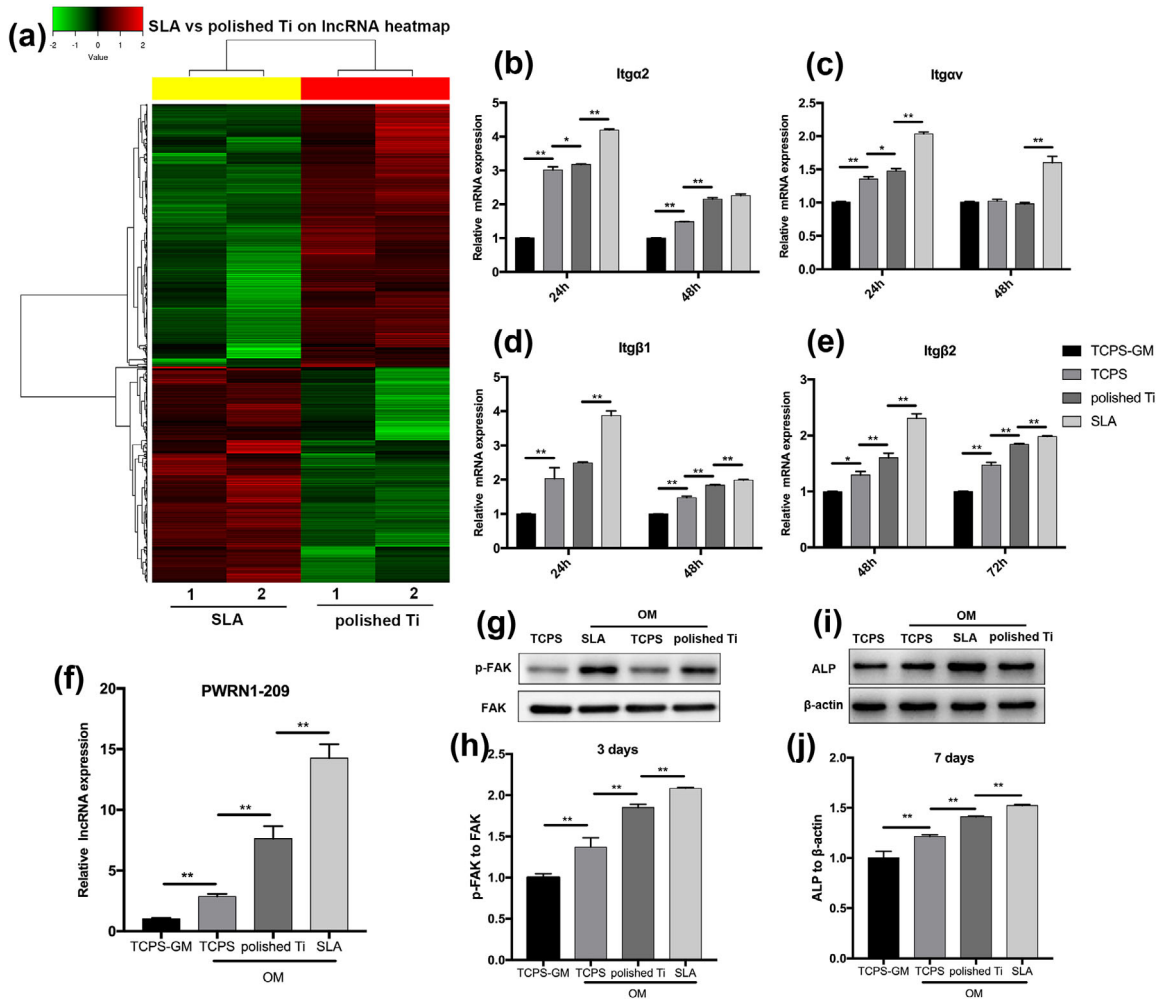

FIGURE 7 Differential expression of PWRN1-209 and consistency with the expression trend of integrins and FAK on several topography surfaces after osteoinducion. (a) Clustering heat map of 1132 differentially expressed lncRNAs analyzed by microarray analysis of hBMSCs cultured on SLA versus polished Ti in osteogenic induction medium (OM) at 7 days. (b–e) The mRNA expression levels of integrins α2, αv, β1, β2 by hBMSCs in the four groups of hBMSCs. (F) The expression level of lncRNA PWRN1-209 in four groups of hBMSCs. (g,h) FAK and p-FAK protein expression in four groups of hBMSCs at day 3. (i,j) ALP protein expression in four groups of hBMSCs at day 7. Error bars are the mean ± *SD*, $^{*}p < 0.05$; $^{**}p < 0.01$, $n = 3$

In this study, we analyzed lncRNA expression from the lncRNA microarray of hBMSCs before and after osteogenic induction on SLA for 7 and 21 days. We identified 4112 differentially expressed lncRNAs in hBMSCs on the SLA Ti surface, of which 2858 lncRNAs were upregulated and 1254 lncRNAs were downregulated at 7 days, and only 1437 lncRNAs were upregulated or downregulated at 21 days. These results suggest that some lncRNAs may have a connection with hBMSC early-stage osteogenic differentiation. We verified the top 10 uncharacterized upregulated lncRNAs at 7 days, and only one novel lncRNA, PWRN1-209, was finally identified. In addition, from the microarray data at 21 days, the expression level of PWRN1-209 was not significantly different, so the effect of PWRN1-209 on MSCs may be in the stage of early osteogenic differentiation. The change tendency was also related to integrins, FAK and ALP on surfaces with different roughnesses. This lncRNA may play a role as a positive regulator of osteogenic differentiation in early osteogenic differentiation and can be upregulated by titanium and microtopography, suggesting that enhanced osteogenic differentiation of microtopography SLA titanium is possibly associated with lncRNA and FAK-ALP signaling.

HBMSCs are derived from mesoderm cell lines that show self-renewal and multidirectional differentiation potential. They can differentiate into a variety of mesenchymal cell types, including osteoblasts and chondrocytes (Rastegar et al., 2010). This process is affected by the interface characteristics in contact with cells. Ti and its alloys have been widely used in dental implants and orthopedic implants due to their good mechanical properties, chemical stability and biocompatibility. Compared with a smooth surface, a moderately rough Ti surface (Sa of 1–2 μm) promotes osseointegration because of its microscale surface topography (Andrukhov et al., 2016; Shaoki et al., 2016; Vlacic-Zischke, Hamlet, Friis, Tonetti, & Ivanovski, 2011; Wennerberg & Albrektsson, 2009). Common methods for roughening

the surface of Ti include plasma spraying, anodizing, sand blasting, acid etching or sand blasting and acid etching (Annunziata & Guida, 2015). SLA implants with microtopography are the most commonly used implants in the clinic. Existing studies have shown that rough surfaces can promote osseointegration, which is related to the microtopography of the material surface and can promote the adhesion and differentiation of MSCs (Huang et al., 2017; Zou et al., 2019).

Our group first characterized the expression profile of lncRNAs in hBMSCs on the classical microtopography SLA titanium surface by microarrays, and a novel lncRNA was screened on the plastic surface, which promoted early-stage osteogenic differentiation of BMSCs. Previous studies showed that there were differences in the expression of numerous proteins on the surface of materials with nano/microtopography, smooth and plastic surfaces, indicating that there may be many reasons for the changing expression of lncRNAs on SLA Ti after stem cell osteogenesis (Barbara, 2001; Wall et al., 2009). Some were merely related to the identification of interface materials, which means topographical surface features are detected by a variety of mechanosensory mechanisms, including integrin binding and focal adhesion formation, leading to cascades of biochemical signals (Wang, Tytell, & Ingber, 2009). A number of lncRNAs may regulate osteogenic differentiation through bone morphogenetic protein (BMP) and Wnt signaling pathways. A more stable screening is needed; therefore, we choose to select the genes related to osteogenic differentiation closely on TCPS instead of titanium, which also explains that although thousands of lncRNAs are upregulated during BMSC osteogenic differentiation on the SLA Ti surface, numerous lncRNAs failed to affect the osteogenic differentiation process in the results. Therefore, this newly discovered lncRNA, PWRN1-209, should have a strong relationship with hBMSC osteogenic differentiation.

ENST00000566676.1 is also called PWRN1-209 in Gene Ensembl (http://asia.ensembl.org/). LncRNA PWRN1 is located in the Prader-Willi syndrome (PWS) region of chromosome 15, which is known to undergo imprinting. Based on bioinformatics analysis and experimental verification, we found that the expression level of PWRN1-209 was upregulated after osteogenic differentiation and that the expression level on microtopography SLA was increased compared to that on polished Ti. According to the latest research, lncRNA PWRN1-211 inhibits the development of gastric cancer through the p53 signaling pathway (Chen et al., 2018). Nevertheless, the exact role and mechanism of PWRN1 in regulating osteogenic differentiation has not been explored.

PWRN1-209 was differentially expressed after osteoinduction on TCPS, further indicating that this lncRNA is involved in the osteogenic reconstruction process, and the difference in polished titanium and SLA may be related to SLA-enhanced osteogenic differentiation (Figure 7f). In this study, we found that PWRN1-209 affected the expression of many osteogenic differentiation genes, alkaline phosphatase is a commonly used marker of early osteogenic differentiation that is triggered by cell contact with ECM, and it can be observed repeatedly to increase in cells adhered to rough surface topography (Martin et al., 1995; Zinger et al., 2005). PWRN1-209 has significant effects on Col1a1 mRNA expression and other bone matrix components (e.g., Bsp). While the lncRNA did not affect the osteogenic transcription factor Runx2, the mechanism by which PWRN1-209 regulates osteogenic differentiation did not involve changes in Runx2 expression. The main studies on the effects of microtopography SLA promoting osteointegration include hydrophilic proteolytic properties, cell adhesion, or cell signal transduction due to mechanical forces (Calciolari, Hamlet, Ivanovski, & Donos, 2018; Klein et al., 2013). Rene and coworkers suggested a major role of the integrin β1 subunit in roughness recognition (Olivares-Navarrete et al., 2015). Additional studies have revealed that particular signals are mediated from topographically modified titanium substrates to cells via integrins, including α2β1 integrin (Olivares-Navarrete et al., 2008). FAK is a key factor involved in the integrin signaling pathway by activating downstream signaling molecules and regulating cytoskeletal structure and cell adhesion, migration, proliferation, and differentiation. Laura and coworkers suggested a mechanism whereby machanotransduction driven by FAK is essential for stem cell growth and functioning on metallic substrates (Saldana, Crespo, Bensiamar, Arruebo, & Vilaboa, 2014). Integrins play an important role in regulating ECM-related hMSC osteogenic differentiation through FAK-extracellular signal-related kinase (ERK) signaling, which can regulate the activity of ALP (Salasznyk, Klees, Williams, Boskey, & Plopper, 2007; Takeuchi et al., 1997). According to our results, the changed trend of lncRNA PWRN1-209 was also related to integrins, FAK, and ALP on surfaces with diverse roughness (Figure 7f–j). The changes in Runx2 that vanished were considered to be influenced by FAK-ERK1/2 downregulation or upregulation (Salasznyk et al., 2007). We speculate that the dramatic alteration in the mRNA expression of Alp may mainly be related to the regulation of FAK by upregulating the expression of ERK-dependent Alp activity to promote osteogenic differentiation of BMSCs (Takeuchi et al., 1997).

Combined with previous studies and the results on the surface of different topography in our study, lncRNA PWRN1-209 is likely to be first involved in recognizing rough topography and is affected by integrin-FAK-ERK to regulate the expression of ALP in cells in response to topography-related osteogenic differentiation.

Our current research still has certain limitations, as only in vitro cell experiments were performed, and more research is needed to validate the exact regulatory mechanisms of lncRNA PWRN1-209 in osteogenic differentiation and topography regulation. Further detailed research needs to be performed to confirm the molecular signals involved. Above all, this study demonstrated the crucial role of PWRN1 in promoting osteogenic differentiation of hBMSCs and the possibility of participating in the process that enhanced osteogenic differentiation of microtopography SLA through integrin-FAK signaling. Our research not only provides a broad mechanism for stem cell osteogenic differentiation but also provides new ideas for surface modification of implants, as well as many therapeutic applications for tissue engineering and regenerative nanomedicine. Moreover, in the process of osteogenesis, many changes in lncRNAs may not have a clear function in osteogenesis. Our work has a high degree of refinement, which is meanful to screen out a lncRNA that is clearly related to osteogenic differentiation of stem cells on the microtopography

SLA surface and then explore its mechanisms of action. Therefore, it is of certain significance to perform this screening. By deeply digging at different stages and under different osteoinduction conditions, the changes in lncRNA may be quite sensitive and may be used to monitor or predict a particular stage in bone formation or osseointegration process for the future. Further detailed research on these roles is necessary and is in progress.

5 | CONCLUSIONS

In conclusion, differential lncRNAs on the microtopography SLA surface after osteoinduction were found via lncRNA microarray and bioinformatics. Functional verification assays demonstrated that lncRNA PWRN1-209 enhances ALP activity and osteogenesis-related marker expression in hBMSCs. This lncRNA can be upregulated by titanium and microtopography and is involved in SLA-enhanced osteogenic differentiation. The change trend of integrins and FAK had a certain correlation with PWRN1-209, and the expression of integrins and the phosphorylation of FAK were increased on SLA with microtopography. Our findings preliminarily revealed that lncRNA PWRN1-209 upregulated by the microtopography surface may facilitate osteogenic differentiation of hBMSCs on the SLA Ti surface and may be related to integrin-FAK-ALP signaling, providing new insights into the molecular mechanisms behind the influence of surface topography on osseointergration or bone formation, which helps us understand the role of the implant surface in regulating cellular responses during complex osseointegration and the effect of lncRNA in cells on the surface topography of implants.

ACKNOWLEDGEMENTS

M. W.: performed the experiments and wrote the paper; X. G., Y. Z., and C. W.: collection and/or assembly of data; Y. Z. and Y. L.: conception and design, financial support, manuscript writing, and final approval of manuscript. This study was financially supported by the National Key R&D Program of China (2018YFC1105302, 2018YFC1105304), the Science Foundation of Peking University School and the Hospital of Stomatology (PKUSS) (grant number 20150106).

CONFLICT OF INTEREST

The authors declare no potential conflict of interest.

REFERENCES

Albrektsson, T., Brånemark, P. I., Hansson, H. A., & Lindström, J. (1981). Osseointegrated titanium implants:Requirements for ensuring a long-lasting, direct bone-to-implant Anchorage in man. *Acta Orthopaedica Scandinavica*, *52*(2), 155–170.

Andrukhov, O., Huber, R., Shi, B., Berner, S., Rausch-Fan, X., Moritz, A., … Schedle, A. (2016). Proliferation, behavior, and differentiation of osteoblasts on surfaces of different microroughness. *Dental Materials: Official Publication of the Academy of Dental Materials*, *32*(11), 1374–1384.

Annunziata, M., & Guida, L. (2015). The effect of titanium surface modifications on dental implant Osseointegration. Biomaterials for Oral and Craniomaxillofacial applications. *Frontiers of Oral Biology*, *17*, 62–77.

Barbara, D. (2001). Boyan, Christoph H Lohmann, David D Dean, victor L Sylvia, David L Cochran, Schwartz Z. mechanisms involved in osteoblast response to implant surface morphology. *Annual Review of Materials Research*, *31*(1), 357–371.

Batista, P. J., & Chang, H. Y. (2013). Long noncoding RNAs: Cellular address codes in development and disease. *Cell*, *152*(6), 1298–1307.

Bornstein, M. M., Valderrama, P., Jones, A. A., Wilson, T. G., Seibl, R., & Cochran, D. L. (2008). Bone apposition around two different sandblasted and acid-etched titanium implant surfaces: A histomorphometric study in canine mandibles. *Clinical Oral Implants Research*, *19*(3), 233–241.

Boyan, B. D., Lossdorfer, S., Wang, L., Zhao, G., Lohmann, C. H., Cochran, D. L., & Schwartz, Z. (2003). Osteoblasts generate an osteogenic microenvironment when grown on surfaces with rough microtopographies. *European Cells & Materials*, *6*, 22–27.

Branemark, P. I. (1983). Osseointegration and its experimental background. *The Journal of Prosthetic Dentistry*, *50*(3), 399–410.

Cai, K., Bossert, J., & Jandt, K. D. (2006). Does the nanometre scale topography of titanium influence protein adsorption and cell proliferation? *Colloids and Surfaces. B, Biointerfaces*, *49*(2), 136–144.

Calciolari, E., Hamlet, S., Ivanovski, S., & Donos, N. (2018). Pro-osteogenic properties of hydrophilic and hydrophobic titanium surfaces: Crosstalk between signalling pathways in in vivo models. *Journal of Periodontal Research*, *53*(4), 598–609.

Chen, Z., Ju, H., Yu, S., Zhao, T., Jing, X., Li, P., … Li, Y. (2018). Prader-Willi region non-protein coding RNA 1 suppressed gastric cancer growth as a competing endogenous RNA of miR-425-5p. *Clinical Science (London, England)*, *132*(9), 1003–1019.

Fatica, A., & Bozzoni, I. (2014). Long non-coding RNAs: New players in cell differentiation and development. *Nature Reviews Genetics*, *15*(1), 7–21.

Galli, C., Passeri, G., Ravanetti, F., Elezi, E., Pedrazzoni, M., & Macaluso, G. M. (2010). Rough surface topography enhances the activation of Wnt/beta-catenin signaling in mesenchymal cells. *Journal of Biomedical Materials Research. Part A*, *95*(3), 682–690.

Garcia, A. J. (2005). Get a grip: Integrins in cell-biomaterial interactions. *Biomaterials*, *26*(36), 7525–7529.

Gittens, R. A., McLachlan, T., Olivares-Navarrete, R., Cai, Y., Berner, S., Tannenbaum, R., … Boyan, B. D. (2011). The effects of combined micron −/submicron-scale surface roughness and nanoscale features on cell proliferation and differentiation. *Biomaterials*, *32*(13), 3395–3403.

Huang, J., Zhang, X., Yan, W., Chen, Z., Shuai, X., Wang, A., & Wang, Y. (2017). Nanotubular topography enhances the bioactivity of titanium implants. *Nanomedicine*, *13*(6), 1913–1923.

Huang, Y., Zheng, Y., Jia, L., & Li, W. (2015). Long noncoding RNA H19 promotes osteoblast differentiation via TGF-beta1/Smad3/HDAC signaling pathway by deriving miR-675. *Stem Cells (Dayton, Ohio)*, *33*(12), 3481–3492.

Huarte, M. (2015). The emerging role of lncRNAs in cancer. *Nature Medicine*, *21*(11), 1253–1261.

J-h, Y., Yang, F., Wang, F., Ma, J.-z., Guo, Y.-j., Q-f, T., … S-h, S. (2014). A long noncoding RNA activated by TGF-β promotes the invasion-metastasis Cascade in hepatocellular carcinoma. *Cancer Cell*, *25*(5), 666–681.

Jin, Z., Yan, X., Shen, K., Fang, X., Zhang, C., Ming, Q., … Cai, K. (2019). TiO2 nanotubes promote osteogenic differentiation of mesenchymal stem cells via regulation of lncRNA CCL3-AS. *Colloids and Surfaces. B, Biointerfaces*, *181*, 416–425.

Klein, M. O., Bijelic, A., Ziebart, T., Koch, F., Kämmerer, P. W., Wieland, M., … Al-Nawas, B. (2013). Submicron scale-structured hydrophilic titanium surfaces promote early osteogenic gene response for cell adhesion and cell differentiation. *Clinical Implant Dentistry and Related Research*, *15*(2), 166–175.

Li, G., Song, Y., Shi, M., Du, Y., Wang, W., & Zhang, Y. (2017). Mechanisms of Cdc42-mediated rat MSC differentiation on micro/nano-textured topography. *Acta Biomaterialia*, *49*, 235–246.

Li, X., Wu, Z., Fu, X., & Han, W. (2014). lncRNAs: Insights into their function and mechanics in underlying disorders. *Mutation Research, Reviews in Mutation Research*, *762*, 1–21.

Liu, Y. K., Uemura, T., Nemoto, A., Yabe, T., Fujii, N., Ushida, T., & Tateishi, T. (1997). Osteopontin involvement in integrin-mediated cell signaling and regulation of expression of alkaline phosphatase during early differentiation of UMR cells. *FEBS Letters*, *420*(1), 112–116.

Martin, J. Y., Schwartz, Z., Hummert, T. W., Schraub, D. M., Simpson, J., Lankford, J., Jr., … Boyan, B. D. (1995). Effect of titanium surface roughness on proliferation, differentiation, and protein synthesis of human osteoblast-like cells (MG63). *Journal of Biomedical Materials Research*, *29*(3), 389–401.

Olivares-Navarrete, R., Raz, P., Zhao, G., Chen, J., Wieland, M., Cochran, D. L., … Schwartz, Z. (2008). Integrin alpha2beta1 plays a critical role in osteoblast response to micron-scale surface structure and surface energy of titanium substrates. *Proceedings of the National Academy of Sciences of the United States of America*, *105*(41), 15767–15772.

Olivares-Navarrete, R., Rodil, S. E., Hyzy, S. L., Dunn, G. R., Almaguer-Flores, A., Schwartz, Z., & Boyan, B. D. (2015). Role of integrin subunits in mesenchymal stem cell differentiation and osteoblast maturation on graphitic carbon-coated microstructured surfaces. *Biomaterials*, *51*, 69–79.

Raines, A. L., Berger, M. B., Schwartz, Z., & Boyan, B. D. (2019). Osteoblasts grown on microroughened titanium surfaces regulate angiogenic growth factor production through specific integrin receptors. *Acta Biomaterialia*, *97*, 578–586.

Rastegar, F., Shenaq, D., Huang, J., Zhang, W., Zhang, B. Q., He, B. C., … He, T. C. (2010). Mesenchymal stem cells: Molecular characteristics and clinical applications. *World J Stem Cells*, *2*(4), 67–80.

Salasznyk, R. M., Klees, R. F., Williams, W. A., Boskey, A., & Plopper, G. E. (2007). Focal adhesion kinase signaling pathways regulate the osteogenic differentiation of human mesenchymal stem cells. *Experimental Cell Research*, *313*(1), 22–37.

Saldana, L., Crespo, L., Bensiamar, F., Arruebo, M., & Vilaboa, N. (2014). Mechanical forces regulate stem cell response to surface topography. *Journal of Biomedical Materials Research. Part A*, *102*(1), 128–140.

Sartori, E., Magro-Filho, O., Mendonça, D., Li, X., Fu, J., & Mendonça, G. (2018). Modulation of micro RNA expression and osteoblast differentiation by Nanotopography. *The International Journal of Oral & Maxillofacial Implants*, *33*(2), 269–280.

Shaoki, A., Xu, J.-Y., Sun, H., Chen, X.-S., Ouyang, J., Zhuang, X.-M., & Deng, F.-L. (2016). Osseointegration of three-dimensional designed titanium implants manufactured by selective laser melting. *Biofabrication*, *8*(4).

Shin, Y. C., Pang, K. M., Han, D. W., Lee, K. H., Ha, Y. C., Park, J. W., … Lee, J. H. (2019). Enhanced osteogenic differentiation of human mesenchymal stem cells on Ti surfaces with electrochemical nanopattern formation. *Materials Science & Engineering. C, Materials for Biological Applications*, *99*, 1174–1181.

Szmukler-Moncler, S., Perrin, D., Ahossi, V., Magnin, G., & Bernard, J. P. (2004). Biological properties of acid etched titanium implants: Effect of sandblasting on bone anchorage. *Journal of Biomedical Materials Research Part B, Applied Biomaterials*, *68*(2), 149–159.

Takeuchi, Y., Suzawa, M., Kikuchi, T., Nishida, E., Fujita, T., & Matsumoto, T. (1997). Differentiation and transforming growth factor-beta receptor down-regulation by collagen-alpha2beta1 integrin interaction is mediated by focal adhesion kinase and its downstream signals in murine osteoblastic cells. *The Journal of Biological Chemistry*, *272*(46), 29309–29316.

Tang, S., Xie, Z., Wang, P., Li, J., Wang, S., Liu, W., … Shen, H. (2019). LncRNA-OG promotes the osteogenic differentiation of bone marrow-derived mesenchymal stem cells under the regulation of hnRNPK. *Stem Cells (Dayton, Ohio)*, *37*(2), 270–283.

Tang, Z., Gong, Z., & Sun, X. (2018). LncRNA DANCR involved osteolysis after total hip arthroplasty by regulating FOXO1 expression to inhibit osteoblast differentiation. *Journal of Biomedical Science*, *25*(1), 4.

Vlacic-Zischke, J., Hamlet, S. M., Friis, T., Tonetti, M. S., & Ivanovski, S. (2011). The influence of surface microroughness and hydrophilicity of titanium on the up-regulation of TGFbeta/BMP signalling in osteoblasts. *Biomaterials*, *32*(3), 665–671.

Wall, I., Donos, N., Carlqvist, K., Jones, F., & Brett, P. (2009). Modified titanium surfaces promote accelerated osteogenic differentiation of mesenchymal stromal cells in vitro. *Bone*, *45*(1), 17–26.

Wang, N., Tytell, J. D., & Ingber, D. E. (2009). Mechanotransduction at a distance: Mechanically coupling the extracellular matrix with the nucleus. *Nature Reviews. Molecular Cell Biology*, *10*(1), 75–82.

Wang, Q., Li, Y., Zhang, Y., Ma, L., Lin, L., Meng, J., … Zhang, Y. (2017). LncRNA MEG3 inhibited osteogenic differentiation of bone marrow mesenchymal stem cells from postmenopausal osteoporosis by targeting miR-133a-3p. *Biomedicine & Pharmacotherapy*, *89*, 1178–1186.

Wang, W., Liu, Q., Zhang, Y., & Zhao, L. (2014). Involvement of ILK/-ERK1/2 and ILK/p38 pathways in mediating the enhanced osteoblast differentiation by micro/nanotopography. *Acta Biomaterialia*, *10*(8), 3705–3715.

Wang, W., Zhao, L., Ma, Q., Wang, Q., Chu, P. K., & Zhang, Y. (2012). The role of the Wnt/β-catenin pathway in the effect of implant topography on MG63 differentiation. *Biomaterials*, *33*(32), 7993–8002.

Wennerberg, A., & Albrektsson, T. (2009). Effects of titanium surface topography on bone integration: A systematic review. *Clinical Oral Implants Research*, *20*, 172–184.

Wu, J., Zhao, J., Sun, L., Pan, Y., Wang, H., & Zhang, W. B. (2018). Long non-coding RNA H19 mediates mechanical tension-induced osteogenesis of bone marrow mesenchymal stem cells via FAK by sponging miR-138. *Bone*, *108*, 62–70.

Wu, Z., Liu, X., Liu, L., Deng, H., Zhang, J., Xu, Q., … Ji, A. (2014). Regulation of lncRNA expression. *Cellular & Molecular Biology Letters*, *19*(4), 561–575.

Yang, Q., Jia, L., Li, X., Guo, R., Huang, Y., Zheng, Y., & Li, W. (2018). Long noncoding RNAs: New players in the osteogenic differentiation of bone marrow- and adipose-derived mesenchymal stem cells. *Stem Cell Reviews and Reports*, *14*(3), 297–308.

Yang, Y., Wang, K., Gu, X., & Leong, K. W. (2017). Biophysical regulation of cell behavior—Cross talk between substrate stiffness and Nanotopography. *Engineering*, *3*(1), 36–54.

Zhang, J., Tao, Z., & Wang, Y. (2018). Long noncoding RNA DANCR regulates the proliferation and osteogenic differentiation of human bone-derived marrow mesenchymal stem cells via the p38 MAPK pathway. *International Journal of Molecular Medicine*, *41*(1), 213–219.

Zhang, W., Dong, R., Diao, S., Du, J., Fan, Z., & Wang, F. (2017). Differential long noncoding RNA/mRNA expression profiling and functional network analysis during osteogenic differentiation of human bone marrow mesenchymal stem cells. *Stem Cell Research & Therapy*, *8*(1), 30.

Zhuang, Q., Ye, B., Hui, S., Du, Y., Zhao, R. C., Li, J., … Zhang, J. (2018). Long noncoding RNA lncAIS downregulation in mesenchymal stem cells is implicated in the pathogenesis of adolescent idiopathic scoliosis. *Cell Death and Differentiation*, *26*(9), 1700–1715.

Zhuang, W., Ge, X., Yang, S., Huang, M., Zhuang, W., Chen, P., … Li, B. (2015). Upregulation of lncRNA MEG3 promotes osteogenic differentiation of mesenchymal stem cells from multiple myeloma patients by targeting BMP4 transcription. *Stem Cells (Dayton, Ohio)*, *33*(6), 1985–1997.

Zhuang, X.-M., Zhou, B., & Yuan, K.-F. (2019). Role of p53 mediated miR-23a/CXCL12 pathway in osteogenic differentiation of bone mesenchymal stem cells on nanostructured titanium surfaces. *Biomedicine & Pharmacotherapy*, *112*.

Zinger, O., Zhao, G., Schwartz, Z., Simpson, J., Wieland, M., Landolt, D., & Boyan, B. (2005). Differential regulation of osteoblasts by substrate microstructural features. *Biomaterials*, *26*(14), 1837–1847.

Zou, J., Wang, W., Nie, Y., Xu, X., Ma, N., & Lendlein, A. (2019). Microscale roughness regulates laminin-5 secretion of bone marrow mesenchymal stem cells. *Clinical Hemorheology and Microcirculation*, *73*, 237–247.

SUPPORTING INFORMATION

Additional supporting information may be found online in the Supporting Information section at the end of this article.

How to cite this article: Wang M, Ge X, Zheng Y, Wang C, Zhang Y, Lin Y. Microarray analysis reveals that lncRNA PWRN1-209 promotes human bone marrow mesenchymal stem cell osteogenic differentiation on microtopography titanium surface in vitro. *J Biomed Mater Res*. 2020;108B: 2889–2902. https://doi.org/10.1002/jbm.b.34620